The Diurnal Cycle of Winds, Rain, and Clouds over Taiwan during the Mei-Yu, Summer, and Autumn Rainfall Regimes

BRANDON WESLEY JOHN KERNS* AND YI-LENG CHEN

Department of Meteorology, School of Ocean and Earth Science and Technology, University of Hawaii at Manoa, Honolulu, Hawaii

MEI-YU CHANG

Central Weather Bureau, Taipei, Taiwan

(Manuscript received 15 April 2009, in final form 20 August 2009)

ABSTRACT

The diurnal variations in surface winds, rain, and clouds over Taiwan are presented for three rainfall regimes: the mei-yu (16 May–15 June), summer (16 July–31 August), and autumn (16 September–15 October). Though the magnitude of diurnal island divergence and convergence is similar under each regime, the diurnal variations of rain and clouds vary considerably between the regimes. These differences are related to the seasonal changes in environment winds, stability, moisture, and weather systems. In addition to orographic lifting on the windward side, rainfall occurrences for all three rainfall regimes are strongly modulated by the diurnal heating cycle with an afternoon maximum. The largest day–night differences in rainfall occur in summer and the smallest differences occur in autumn. The upper-level high cloud (<235 K) frequencies have a pronounced afternoon maximum over the mountainous areas in the afternoon because of combined effects of orographic lifting and solar heating. These clouds are advected downstream by the upper-level winds in late afternoon and early evening. The highest afternoon high cloud frequencies occur in summer (>30%) with the lowest upper-level cloud cover in autumn (~10%). In autumn, most of the orographic showers on the eastern and northeastern windward side in the late afternoon and early evening are not from deep clouds. The weak early-morning rainfall maxima for all three seasons are related to the localized boundary layer convergence due to the orographic blocking of the prevailing winds and their interactions with the offshore/land breeze. During disturbed, prefrontal periods in the mei-yu, bands of high clouds and rain tend to develop in the early morning in the convergence zone off the northwest coast. These rainbands are responsible for the early-morning rainfall maximum on the northwest coast. They do not occur in summer or autumn.

1. Introduction

Taiwan is subject to the northeast monsoon from September to early May, and the southwest monsoon dominates for the rest of the year (Murakami 1958; Ramage 1971; Tao and Chen 1987; Boyle and Chen 1987). The seasonal changes of prevailing wind and atmospheric stability give Taiwan five distinct rainfall regimes:[1] winter, spring, mei-yu, summer, and autumn (Chen and Chen 2003). The autumn, winter, and spring rainfall regimes occur within the northeast monsoon. The mei-yu and summer rainfall regimes occur during the southwest monsoon. In general, the heaviest and most frequent rainfall occurs on the windward side of the island for each regime. However, heavy rainfall (>100 mm day^{-1}, which is likely to cause flash flooding in the steep terrain of Taiwan) is not common in winter and spring because of

* Current affiliation: Rosenstiel School of Marine and Atmospheric Science, University of Miami, Miami, Florida.

Corresponding author address: Dr. Yi-Leng Chen, Department of Meteorology, SOEST, University of Hawaii at Manoa, Honolulu, HI 96822.
E-mail: yileng@hawaii.edu

DOI: 10.1175/2009MWR3031.1

[1] Because of Taiwan's unique location within the East Asian monsoon, the rainfall regimes do not exactly correspond with the four seasons (winter, spring, summer, and autumn) usually discussed in climatology literature.

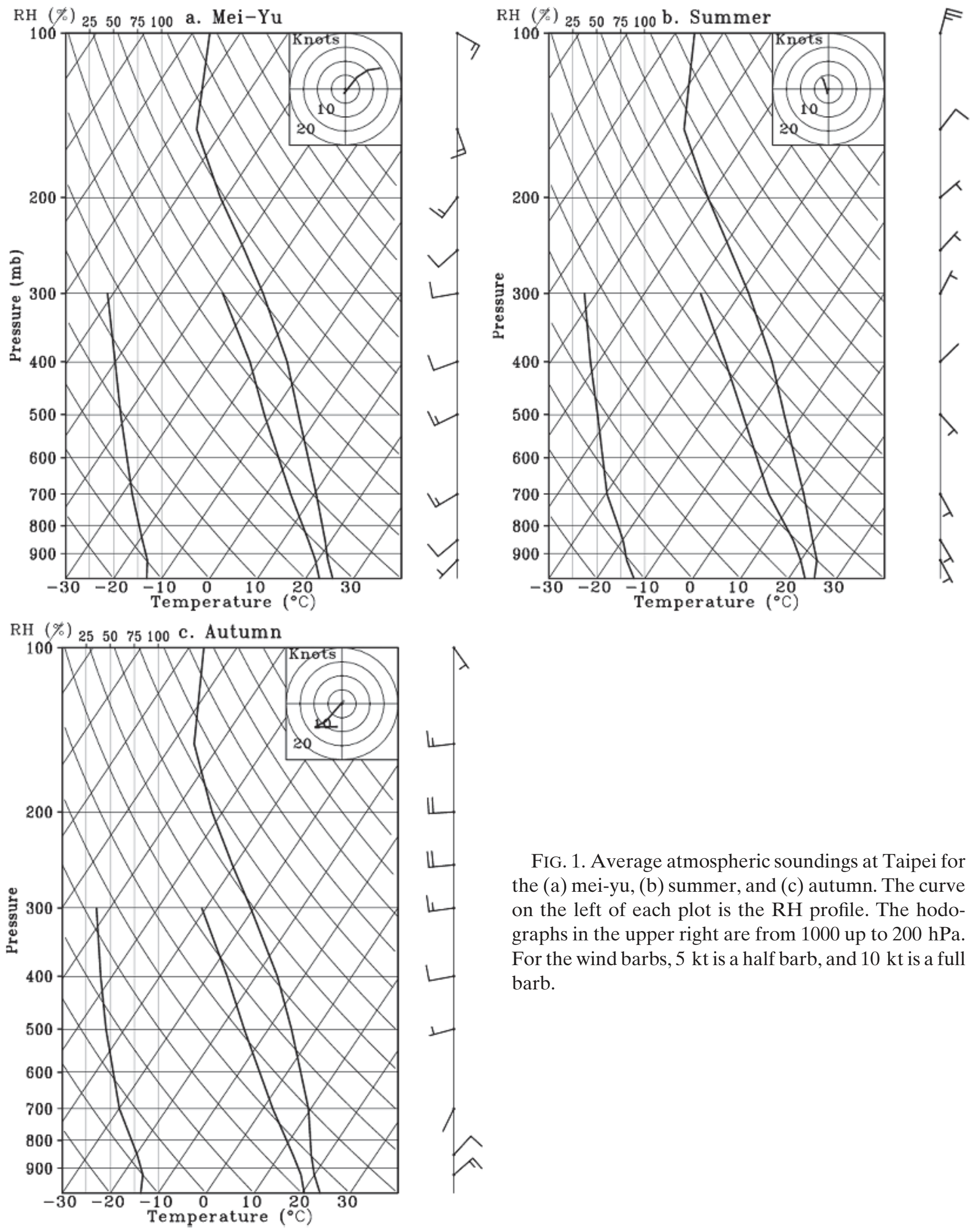

FIG. 1. Average atmospheric soundings at Taipei for the (a) mei-yu, (b) summer, and (c) autumn. The curve on the left of each plot is the RH profile. The hodographs in the upper right are from 1000 up to 200 hPa. For the wind barbs, 5 kt is a half barb, and 10 kt is a full barb.

greater atmospheric stability. Thus, there are three main distinct rainfall regimes over Taiwan: mei-yu (16 May–15 June), summer (15 July–31 August), and autumn (16 September–15 October; Chen and Chen 2003). These three regimes are characterized by different environment flow characteristics, stability, moisture, and embedded weather disturbances.

During the mei-yu regime (16 May–15 June), the mean large-scale flow over Taiwan is characterized by southwesterly flow increasing with height (Figs. 1a and 2a). However, the island experiences wind fluctuations associated with the passage of mei-yu fronts (Chen and Li 1995). The postfrontal cold northeasterlies are generally less than 1 km deep (Chen et al. 1989; Trier et al. 1990). The thermodynamic stratification around Taiwan during the mei-yu is conditionally unstable within the warm, moist southwesterly monsoon flow (Chen and Chen 2003). The combination of low–midlevel wind shear,

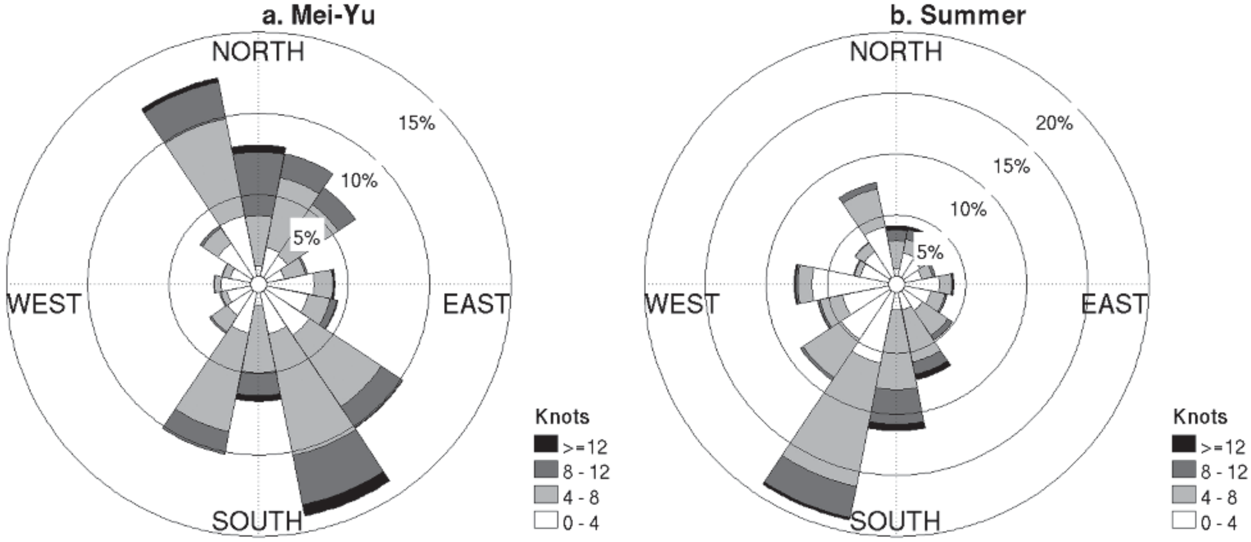

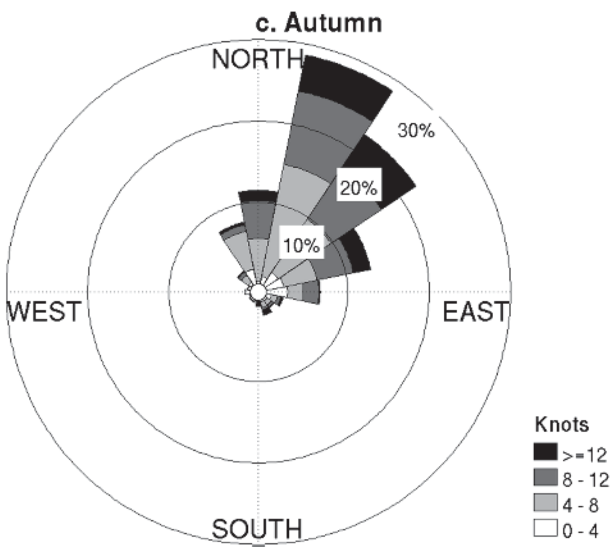

FIG. 2. Wind roses at Penghu for the (a) mei-yu, (b) summer, and (c) autumn. The range rings are relative frequencies of occurrence. The hourly winds are binned according to direction and wind speed (shading).

conditional instability, and abundant moisture favors the formation of organized mesoscale convective systems in the southwest monsoon, especially associated with a mei-yu front (Wang et al. 1990; Lin et al. 1990). Heavy rainfall is most common on the west side of the Central Mountain Range (CMR) during the mei-yu often caused by the interaction of synoptic and subsynoptic weather systems with the terrain of Taiwan (Li et al. 1997; Teng et al. 2000; Chen et al. 2007). However, heavy rainfall can also occur in the northeast part of Taiwan during brief periods following the passage of mei-yu fronts. In some instances, heavy rain could possibly occur merely from the interaction of the terrain and local circulations with the environment flow (Chen et al. 1991; Akaeda et al. 1995).

In mid-June, concurrent with the seasonal change of the upper-level winds from westerlies to northeasterlies over Taiwan, the mei-yu trough migrates northward to the Yangtze River Valley and Japan as the mei-yu regime comes to an end over Taiwan (Chen 1993). After the seasonal change, the upper-level northeasterlies along the southeastern flank of the Tibetan high prevail over Taiwan (Figs. 1b and 2b), preventing most baroclinic systems in the midlatitude westerlies from affecting Taiwan (Chen 1993). Another rainfall peak occurs during 15 July–31 August and is classified as the summer rainy regime over Taiwan (Chen and Chen 2003). Though summer is the most unstable regime considered (Table 1), it is not the peak in annual rainfall for many stations over Taiwan except for the eastern and southeastern areas, where heavy rainfall frequently occurs when a tropical cyclone from the western Pacific moves westward and affects Taiwan (Chen and Chen 2003).

Organized mesoscale systems (aside from tropical cyclones) are less common than in the mei-yu regime. The diurnal cycle in summer is most representative of the influence of the island circulations along with little interaction with the environment.

Autumn occurs after the onset of the northeast monsoon (Figs. 1c and 2c), and it is the most stable regime considered. The low-level environment winds during autumn are the strongest of the three main rainfall regimes. Autumn also features the lowest mean CAPE and positive mean lifted index (LI) (Table 1c). Autumn is the last chance for deep convection before the winter regime sets in with cold surges (Chen and Chen 2003). Rainfall reaches a secondary seasonal peak in the northeast part of Taiwan as this area is on the windward side of the northeasterly monsoon flow.

In addition to large-scale conditions, island-induced flows such as: flow blocking, orographic lifting, and diurnal circulations and their interactions with the large-scale flow also affect the timing and location of rainfall occurrences in a mountainous island like Taiwan and in many different parts of the world (Grossman and Durran 1984; Ogura and Yoshizaki 1988; Oki and Musiake 1994; Akaeda et al. 1995; Li et al. 1997; Li and Chen 1998; Yeh and Chen 1998; Teng et al. 2000; Chen and Chen 2003; Dairaku et al. 2004). Taiwan is an ideal place to study the interactions between the large-scale environment and the local island forcing because of its exposure to a variety of planetary and synoptic-scale weather scenarios and a dense surface observation network. The nature of the local island forcing depends on the prevailing flow and atmospheric stability as well as individual weather disturbances that may affect Taiwan (e.g., squall lines and typhoons). The terrain of Taiwan is dominated by the CMR with average ridge elevation around 2.5 km and peaks above 3 km (Fig. 3). The terrain of Taiwan is a significant obstacle to the low-level flow. With a mean ridge height of $h \sim 2.5$ km, a mean low-level wind speed of 5–10 m s^{-1}, and a Brunt–Väisälä frequency of $\sim$0.01 s^{-1}, the Froude number ($\mathrm{Fr} = U/Nh$) is $\mathrm{Fr} \sim 0.2$–0.4. When $O(\mathrm{Fr}) < 1$, the terrain presents an obstacle to the flow, and flow blocking occurs (Overland and Bond 1995). Similar to the Big Island of Hawaii (Smolarkiewicz et al. 1988), the prevailing flow is blocked by the CMR in Taiwan with leeside vortices (Sun et al. 1991; Sun and Chern 1993).

Ramage (1952) found a strong afternoon maximum over northern Taiwan but weak morning and afternoon maxima in the south, for May–August. The Taiwan Area Mesoscale Experiment (TAMEX) was conducted from 1 May to 29 June 1987 (Kuo and Chen 1990). Johnson and Bresch (1991) found that the early afternoon rainfall maxima occurred at 100–500-m elevation. Yeh and Chen (1998) documented the diurnal cycle of several regions of the island during TAMEX. The diurnal maximum was 1–2 h earlier [starting at 1500 local time (LT)][2] on the windward (west) lower slopes (500–1000-m elevation) than in the high terrain. The diurnal cycle near the southwest and northwest coasts was not pronounced with weak early-morning maxima. On the lee side of Taiwan (east), the diurnal rainfall maximum was delayed until 1700–2000 LT. Note that during TAMEX, there were only 85 hourly rain gauges that are unevenly distributed over Taiwan.

TABLE 1. Mean and std devs of convective indices calculated from soundings taken at Taipei during the (a) mei-yu, (b) summer, and (c) autumn: CAPE (J kg^{-1}), LI (°C), and PW (mm). Note that while the mean LI is slightly positive for the mei-yu, it is negative at nearby stations. During the mei-yu the conditions alternate between unstable prefrontal and stable postfrontal.

	Avg	Std dev
(a) Mei-yu		
CAPE	460	742
LI	0.61	3.8
PW	54	10
(b) Summer		
CAPE	947	790
LI	−2.3	2.2
PW	57	9.3
(c) Autumn		
CAPE	336	497
LI	0.85	3.3
PW	49	10

Krishtawal and Krishnamurti (2001) used rainfall estimated by the Tropical Rainfall Measuring Mission (TRMM) for May–September 1998 to document the diurnal cycle of rainfall over Taiwan. They found a dominant afternoon maximum with secondary morning ($\sim$0600–0700 LT) and nighttime ($\sim$2200–0000 LT) maxima. Furthermore, that study suggested that the TRMM-estimated rainfall in the Taiwan Strait also has a diurnal cycle with a late-night to early-morning maximum.

In 1993, Taiwan's Central Weather Bureau (CWB) installed and began to use the Automatic Rainfall and Meteorological Telemetry System (ARMTS) to aid in flash flood forecasting (Central Weather Bureau 1995; Hsu 1998). Chen et al. (1999) used the ARMTS rain gauges available during 1993–97 and 25 conventional stations over Taiwan to study the rainfall diurnal cycle

[2] Local time is UTC + 8 h. Taiwan does not observe daylight savings time. Local sunrise (sunset) ranges from 0500 (1845) in June to 0600 (1715) by the end of October. Local noon is within 10 min of solar noon, except near the end of October, when solar noon occurs at $\sim$1140 LT.

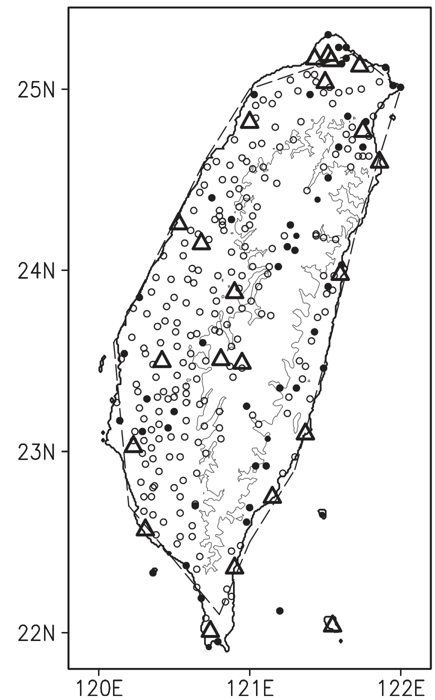

FIG. 3. The terrain of Taiwan and the locations of the ARMTS and conventional stations. Conventional stations are marked with triangles, ARMTS stations with winds and rain are marked with closed circles, and ARMTS stations with rain only are marked with open circles. The terrain contour interval (CI) is 100 m. The dashed line is the integration path used for calculating the island divergence.

averaged over the entire southwest monsoon period (May–August). They found dominant afternoon maxima with secondary morning maxima over the western coastal plain near the mountains. Their analysis of the seasonal cycle showed that stations in the northwest experience rainfall maxima in May (mei-yu) while those over the southwest coastal plain have rainfall maxima in August (summer). However, they did not discuss the diurnal cycle of rainfall of the mei-yu and summer separately. In this study, in addition to island-averaged diurnal rainfall variations, detailed horizontal distributions of diurnal rainfall variations for mei-yu, summer, and autumn rainfall regimes were investigated. The spatial variability of diurnal rainfall variations is affected by the environment flow, the interactions between the environment flow and local winds, and individual weather systems embedded in the flow. The goals of this study are to use the ARMTS database to distinguish between the diurnal wind, rainfall, and cloud patterns characteristic of the mei-yu, summer, and autumn and to study the island effects on rainfall diurnal cycle under different rainfall regimes. Additionally, the diurnal climatology of cold clouds measured by geostationary infrared (IR) satellite data is used to determine the diurnal cycle of cloudiness over the island as well as over the open ocean.

2. Data and methods

a. Hourly rainfall

Figure 3 shows the locations of the ARMTS and conventional stations available for 1997–2002. The coastal plains and terrain below 1000 m are densely covered by the network, but there are limited data above 1000-m elevation. All of the ARMTS and conventional stations measure hourly rainfall at a precision of 0.5 mm. Hourly rainfall is recorded as the rainfall accumulation during the previous hour. Rainfall is measured using tipping-bucket gauges. Further details on the capabilities of the conventional and ARMTS network over Taiwan can be found in the report by the Central Weather Bureau (1995).

Because of instrument malfunction, transmission errors, and quality control, all stations had missing rainfall data at sometime during the study period. To be included in the study, a station had to satisfy a minimum data requirement. Each station was required to have valid rainfall observations for at least 20 days for the mei-yu and autumn and at least 30 days for summer. The data requirement test was done separately for each hour of the diurnal cycle. Some stations consistently had missing data at a particular hour and did not satisfy the data requirements for that hour. However, for other hours the station may have provided sufficient data. The minimum data requirements had to be met for each study year for the station to be included. A zero rainfall observation counts as a valid observation.

For each station, hourly rainfall frequency and hourly rainfall rate were calculated for each hour of the diurnal cycle. These calculations were done independently for the mei-yu, summer, and autumn. Hourly rainfall frequency was computed as the number of days with measurable rainfall (>0.5 mm) in each hour divided by the number of days with observations for that hour. It is expressed as a percent. The hourly rainfall rate is defined as the total rainfall in each hour divided by the number of observations for that hour. Rainfall rate may be strongly affected by heavy rain events not related to the diurnal cycle. For example, a typhoon could contribute a large fraction of the seasonal rainfall at a station over a period of several hours. However, such an event would only contribute a single rainfall occurrence with a small influence on the hourly rainfall frequency. In addition to the individual stations hourly rainfall frequency and rate, the island mean hourly rainfall frequency and rainfall rate were calculated by averaging the hourly rainfall frequency and rate for all of the stations for each hour.

While the afternoon rainfall frequency and rate peak is easy to see in the diurnal composite time series of island mean rainfall frequency and rate, some stations had their rainfall rate and/or frequency maximum during the morning or evening. The time series of rainfall frequency and rain rate were examined qualitatively to determine which stations have diurnal rainfall maxima during the morning and evening transition periods (0700–0800 and 1900–2000 LT, respectively). The maxima at each chosen station were at least 5% above the diurnal mean background for rain frequency and 0.4 mm h^{-1} higher for rain rate for at least 2 consecutive hours ending on the hour. Because the timing of the maxima for hourly rainfall frequency and hourly rain rate may not coincide at exactly the same hour, especially during the transition period, both are presented.

b. *Hourly winds*

Hourly winds are recorded at the conventional stations and at select ARMTS stations as shown in Fig. 3. Winds are measured by the standard wind vane and cup instrumentation with a precision of 0.1 m s^{-1}. Wind observations are recorded as the winds at the particular hour. The ARMTS wind data are of less quality than the conventional station winds. Wind data were used only for days with at least 18 h of wind data, except at four conventional stations (Tanshui, Ilan, Tungchitao, and Yushan, Taiwan) where wind measurements were made only at 0200, 0500, 0800, 0900, 1100, 1400, 1700, 2000, 2100, and 2300 LT for some years. Because the data from these stations are more reliable than the ARMTS measurements, an exception to the 18-h of data day^{-1} rule was granted for these stations.

The hourly mean winds were computed by taking the vector average of all observations for each hour. Wind steadiness, the ratio of the speed of the vector mean wind to the average of the individual wind speeds, was also computed. High wind steadiness indicates that the wind direction is consistent from day to day. Wind steadiness is a better indication of the consistency of the wind direction than the magnitude of the mean wind vector because it is less dependent on wind speed.

Hourly island mean divergence was calculated using the line integral technique with the path illustrated in Fig. 3. For each line segment, the component of the hourly mean wind normal to the segment was multiplied by the length of the segment. The mean divergence within the line integral boundary was obtained by summing all segments and dividing by the total area. The diurnal mean island divergence was subtracted from the hourly divergence.

The surface winds measured at Penghu, Taiwan (23.57°N, 119.56°E, elevation 11 m), within the Taiwan Strait are taken to be representative of the open-ocean low-level flow. Wind roses are presented for this station to depict the dominant low-level environment flow.

c. *Atmospheric soundings*

Routine atmospheric soundings were available at Taipei, Taiwan (25.03°N, 121.51°E). The soundings taken at Taipei may be influenced by local terrain. This is especially relevant for the winds below ~700 hPa. The low-level flow is better depicted using the wind roses from Penghu (23.57°N, 119.56°E).

Several convective indices were computed for each sounding individually and the mean and standard deviations computed. The CAPE and LI were calculated using a parcel with the mean temperature, dewpoint, and pressure from the lowest 500 m of the atmosphere. The precipitable water (PW) was also computed for each sounding. The sounding data were obtained from the University of Wyoming.

d. *Infrared satellite data*

The infrared channel of the *Geostationary Meteorological Satellite-5* (*GMS-5*) was used in this study. These data have been archived and geo-mapped at Kochi University, Japan. Using the IR satellite data from 1997 to 2002, the hourly frequencies (ratio of occurrences to total observations) of high cloud (<235 K) occurrence were computed at each 5 km by 5 km pixel. The 235-K threshold qualitatively represents the products of deep convection (Fu et al. 1990).

3. Rainfall variations and diurnal wind evolution

Rainfall frequencies and rates are overall highest in the mei-yu compared with summer and autumn (Figs. 4 and 5). During the mei-yu, rainfall frequencies are above 30% with averaged rain rates >1 mm h^{-1} over the interior mountains west of the CMR ridgeline (Fig. 4a). Therefore, during the course of the 30-day mei-yu regime these stations receive ~700 mm of rain. This is more than most parts of the western United States receive in an average year. At lower elevations, rainfall frequencies range between 10% and 20% with rain rates of 0.1–0.8 mm h^{-1}. The contrast between the windward and leeward sides, relative to the mean southwesterly flow (Fig. 1a), is not significant. Rainfall tends to occur in the northeast part of Taiwan after the passage of a mei-yu front. After the frontal passage, the winds become northerly for a period of time, which is illustrated by the wind rose in Fig. 2a. In summer, rainfall rates and frequencies are lower than the mei-yu except over southwest

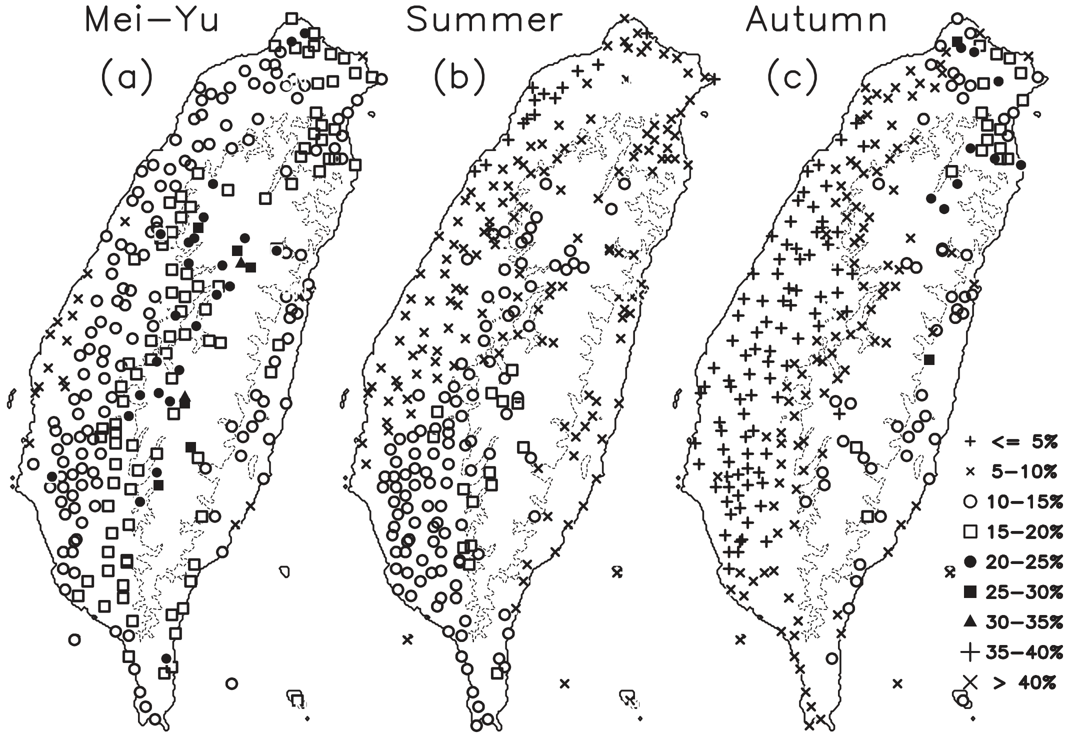

FIG. 4. Rainfall frequencies for the three regimes as a whole: (a) mei-yu, (b) summer, and (c) autumn. The rainfall frequencies are the percentage of all hourly observations made that had measurable rainfall (>0.5 mm).

Taiwan and the mountainous interior (Figs. 4b and 5b). In contrast to the mei-yu, the southwest (windward) side of Taiwan is much rainier than the northeast (lee) side. The persistent southerly wind in summer (Fig. 2b) leads to enhanced rainfall over southwest Taiwan as the warm, moist monsoon flow impinges on the CMR. In autumn, elevated rain frequencies of >15% and rain rates >0.8 mm h^{-1} only occur in the northeast part of Taiwan. Though the environment is more stable in autumn (Fig. 1; Table 1), orographic precipitation occurs in the northeast part of Taiwan due to the persistent and relatively strong northeast monsoon flow (Figs. 1c and 2c).

As expected, the diurnal variation in surface winds is significant under each regime. In general, the offshore–katabatic winds dominate in the early morning and the onshore anabatic flow during the daytime (Figs. 6, 7, and 8). However, the wind steadiness of the onshore and offshore winds varies with location and regime.

For the mei-yu and summer, the early-morning offshore flow is more steady (wind steadiness ≥ 0.7) on the east side of Taiwan than on the west side (~0.5; Figs. 6a and 7a). In contrast, the afternoon onshore–upslope flow has higher wind steadiness on the west side of Taiwan than the east side (Fig. 6c). During the mei-yu, on the west side of Taiwan, the prevailing southwest flow opposes the katabatic flow (Fig. 6a) with flow deceleration and splitting upstream (Chen and Li 1995) at night and complements the anabatic flow in the afternoon (Fig. 6c). For most stations, afternoon sea breezes are relatively strong (>2 m s^{-1}) as compared with nighttime land breezes (0.5–1.5 m s^{-1}). At 1900 LT, the winds along the north and east sides resemble blocking pattern under shallow postfrontal northeasterly flow. At that time, winds are weak over northeast coast with easterly winds over the north shore and northerly winds along the east coast (Fig. 6d). During the evening transition, winds along the southeast coast turn counterclockwise as found by Yeh and Chen (1998). Over northern Taiwan, winds turn clockwise during the evening transition (Figs. 6c,d) and become weak offshore flow around sunrise (Fig. 6a). Summer is closest to undisturbed environment flow, and flow blocking is less important compared with the mei-yu. In summer, the afternoon anabatic winds are most persistent in the northeast part of Taiwan (Fig. 7c). In the mei-yu and summer, the winds are less persistent during the morning and evening transitions than at other times of the day (Figs. 6 and 7), reflecting the fact that the diurnal wind shift may occur at slightly different times under different synoptic conditions.

The wind direction is most persistent in autumn (Fig. 8). Many stations have wind steadiness above 7.0 throughout the diurnal cycle. This is related to the strong persistent

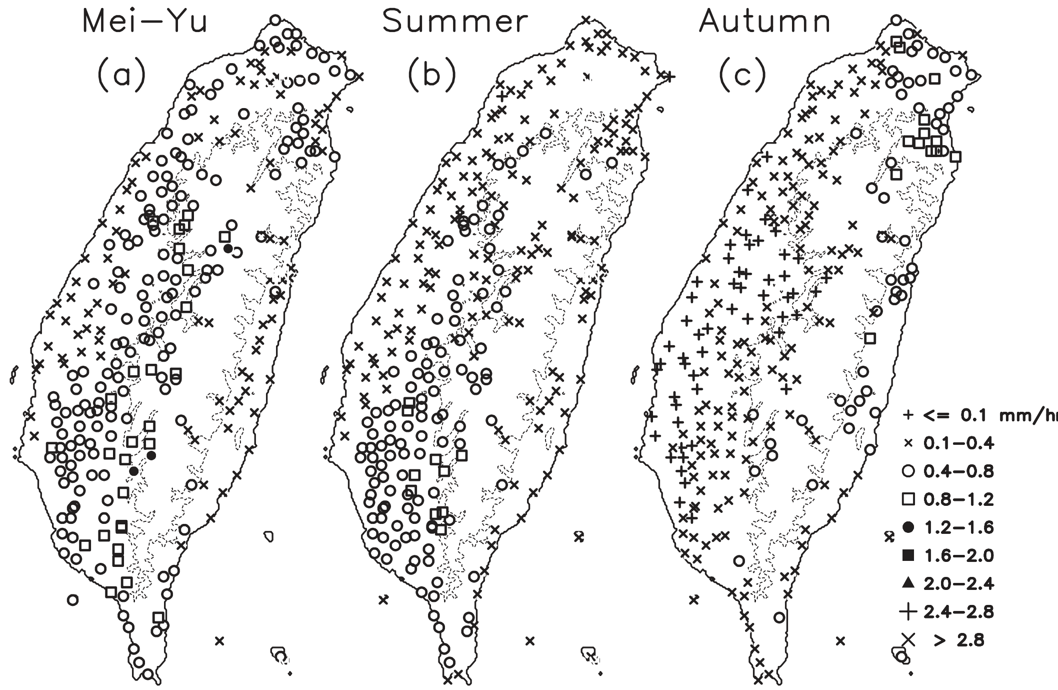

FIG. 5. Mean hourly rain rate for the three regimes as a whole: (a) mei-yu, (b) summer, and (c) autumn. Rain rate is the total rainfall divided by the number of total observations; that it, it is not the conditional rain rate of observations with precipitation.

northeast monsoon flow that prevails in autumn. In autumn, orographic blocking by the prevailing northeasterly monsoon flow is significant and this has an effect on the diurnal wind variations. Over the windward northeastern coast, winds are relatively weak because of orographic blocking. The airflow there exhibits a weak offshore wind component at night with a relatively low steadiness (0.1–0.6) and an onshore wind component during the day. Along the northern Taiwan coast, northeasterly winds are persistent but are the weakest in the early morning when the land surface is the coldest before sunrise. Along the southeastern coast, winds are more or less parallel to the coast with a northerly wind component during the evening and early-morning transitions. Winds there have an offshore wind component at night and an onshore wind component during the day. In the southwest part of Taiwan, wind steadiness is relatively low (<0.6) in the morning, and there are clear diurnal wind shifts. Clearly, the northeast monsoon flow is blocked by the CMR allowing onshore flow to develop in southwest Taiwan in the afternoon. It is shown later that in autumn, the southwest part of Taiwan is the only place where afternoon convection is preferred.

The magnitudes of the maximum morning divergence ($\sim 2 \times 10^{-5}$ s^{-1}) and early afternoon maximum convergence ($\sim -4 \times 10^{-5}$ s^{-1}) are similar to the results of Yeh and Chen (1998) for the 1987 mei-yu (Fig. 9a). There are small seasonal variations in island-scale convergence between the regimes. Similar to the findings of Yeh and Chen (1998) for the mei-yu, the island-averaged rainfall maxima for all three regimes occur in the late afternoon (1600–1700 LT), which is 3 h later than the maximum early afternoon convergence (1300 LT; Figs. 9b,c).[3] The largest day–night differences in rainfall occurrences and rate averaged over the island are observed in summer with the smallest differences in autumn. Autumn is associated with the lowest afternoon peak rainfall frequency and amount and the smallest diurnal amplitudes in rainfall variations. However, the afternoon convergence in autumn is similar to the afternoon convergence during mei-yu and is only slightly smaller than summer. In addition to the development of the onshore/offshore flow in response to the diurnal heating cycle, the rainfall occurrences in Taiwan are also related to stability, moisture, prevailing winds, and large-scale weather patterns. Autumn is associated with less unstable and drier conditions as compared with mei-yu and summer (Table 1). In contrast, the greatest

[3] The minimum statistically significant (0.01 level) hourly difference is 1.8% for rain frequency and 0.09 mm h^{-1} for rain rate. These values were determined somewhat pessimistically using the t test with an assumed sample size of 200 and std devs of 10% and 0.5 mm h^{-1}, respectively.

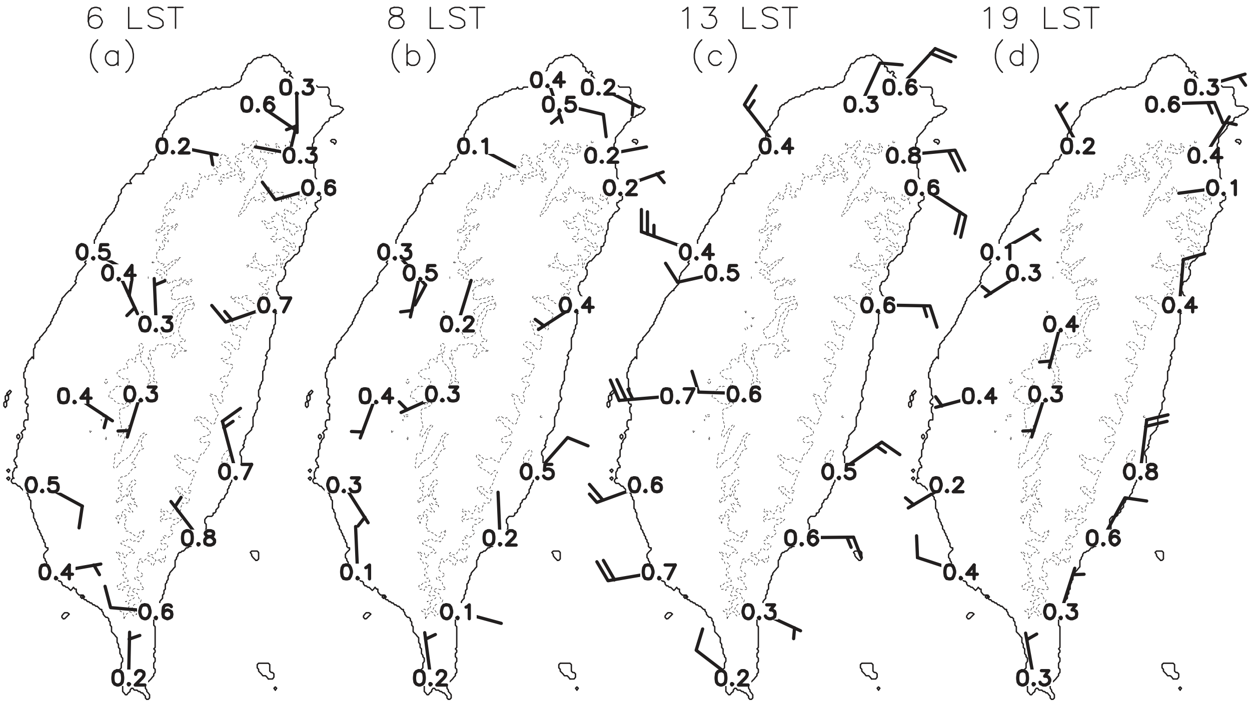

FIG. 6. Mean (1997–2002) winds and wind steadiness at select times during the mei-yu. Half barbs are 0.5 m s^{-1}, full barbs are 1.0 m s^{-1}, and pennants are 5.0 m s^{-1}. The terrain CI is 1000 m. Wind steadiness is given at the stem of each wind barb.

instability is observed in summer with a pronounced afternoon rainfall peak.

Rainfall frequencies and rates are higher during mei-yu than in summer and autumn because of the frequent arrival of the mei-yu fronts over the Taiwan area from southern China (Kuo and Chen 1990; Chen 1993). The enhanced rainfall frequency, rate, and percentage of high cloud in the early morning is not related to island-induced

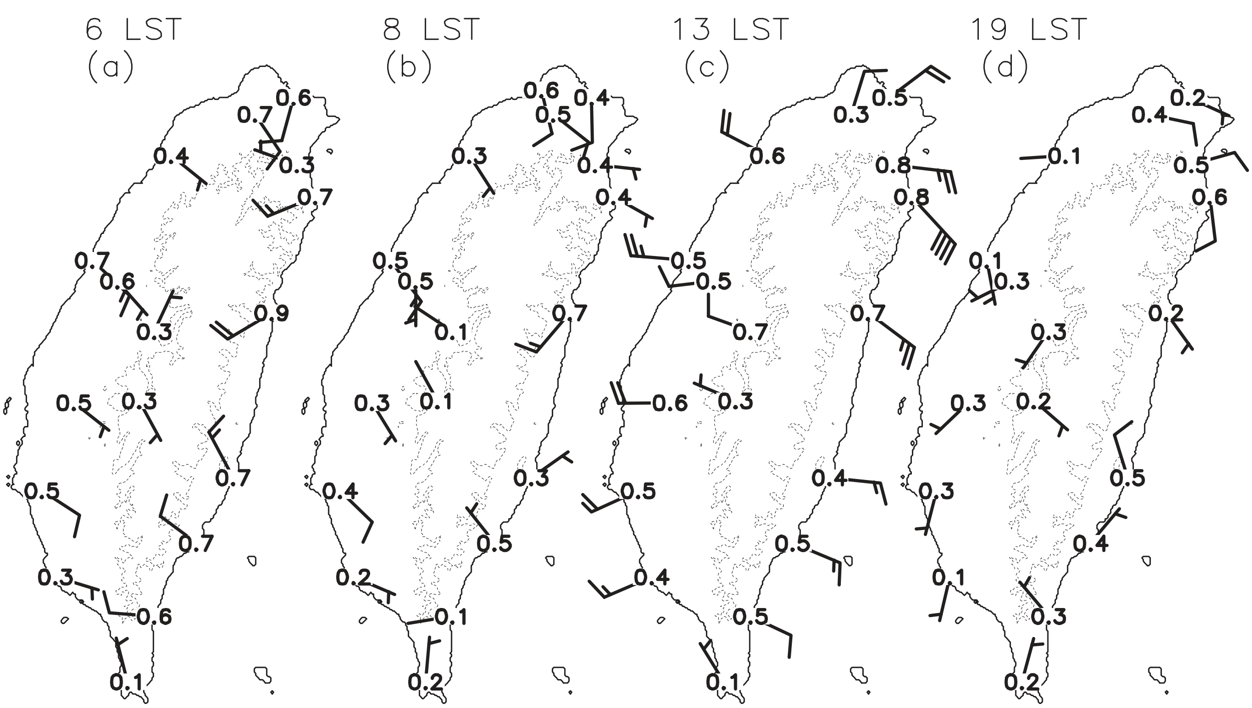

FIG. 7. As in Fig. 4, but for summer.

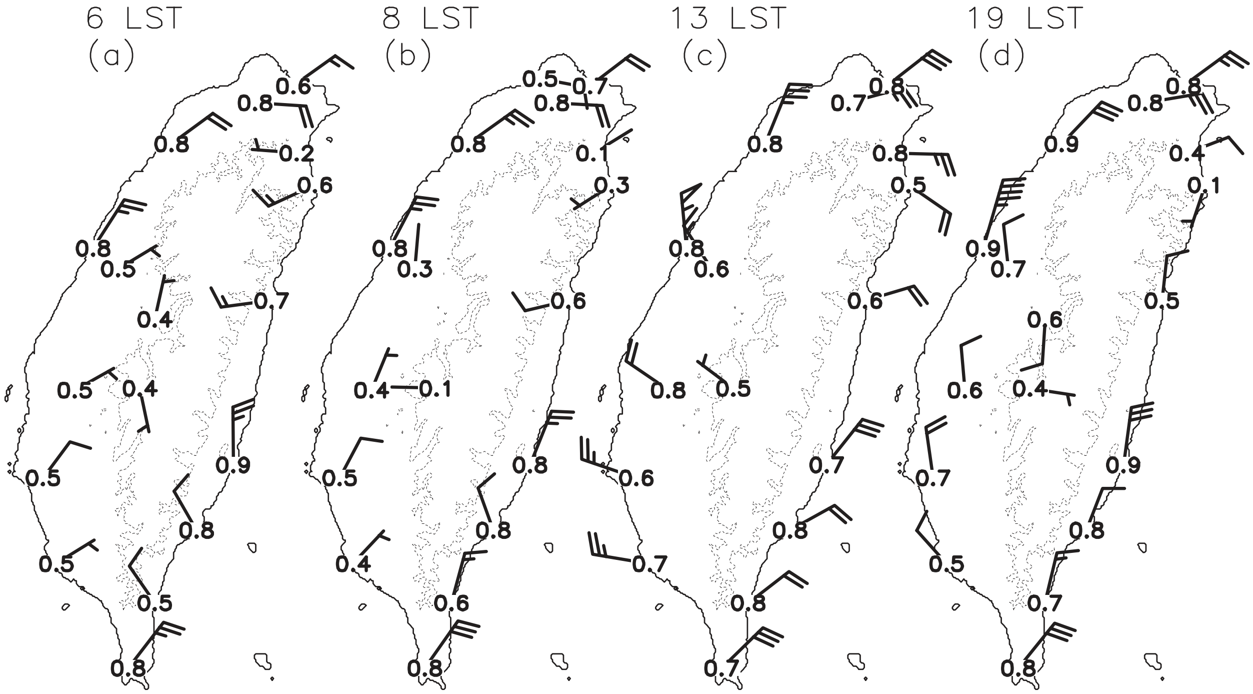

FIG. 8. As in Fig. 4, but for autumn.

convergence. The island circulation is divergent at that time. Instead, it appears to be related to a unique interaction between the environment flow and the CMR, mainly during disturbed periods preceding mei-yu frontal passages. This is discussed further in the next section.

4. Mei-yu

a. Diurnal rainfall patterns

Figure 10 presents the hourly rainfall frequencies over Taiwan for select times of day; the times are chosen to emphasize the contrast between the nighttime and afternoon conditions but also include the transition periods in the early morning and early evening. For most stations, there is a significant afternoon maximum in rainfall occurrence in response to solar heating over land. Except at stations along the west coast, an afternoon rainfall maximum is clearly evident (Fig. 10c) with the highest hourly rainfall frequencies (>40%) in the mountainous terrain during the afternoon maximum. Yeh and Chen (1998) show that more than 50% of rainfall over mountain interior during TAMEX occurred during undisturbed periods as afternoon orographic showers. Maximum afternoon rainfall occurrences are also observed over northern, northeastern, and eastern lower slopes as a result of the development of upslope flow in the afternoon hours. The seasonal mean winds vary throughout Taiwan. The southern half of Taiwan experiences weak mean southwesterly winds, and the northern half of Taiwan experiences weak mean northeasterlies. The weak winds are the average of the postfrontal northeasterlies and the southwest monsoon flow.

At night, rainfall over the western plain, and along the western and eastern coasts, is infrequent (<10%; Fig. 10a). Higher rainfall frequencies (10%–20%) are found over southwestern Taiwan, western slopes, and northern and northeastern Taiwan. Rainfall at night over southern and southwestern Taiwan is mainly due to drifting of rain showers inland under prefrontal southwest monsoon flow and during mei-yu frontal passages. Rainfall over western windward slopes at night is caused by relatively weak orographic showers under disturbed weather. Northern and northeastern Taiwan is on the windward side under the postfrontal northeasterly flow. Rainfall there mainly occurs during and immediately after frontal passages.

After sunrise, rainfall occurrences increase over the coastal plains, western windward lower slopes, and southwest Taiwan. Along the west and northwest coasts, the rainfall frequencies are the highest (10%–15%) in the early morning during the diurnal cycle (Fig. 10b) and relatively low in the afternoon (Fig. 10c). As shown in Figs. 11a,b, several stations on west and northwest Taiwan have a maximum rainfall occurrence during the morning transition (0600–0900 LT). These rainfall maxima occur before the onset of onshore flow and the shifting of island-scale mean divergence to convergence around 0900–1000 LT (Fig. 9a). As will be

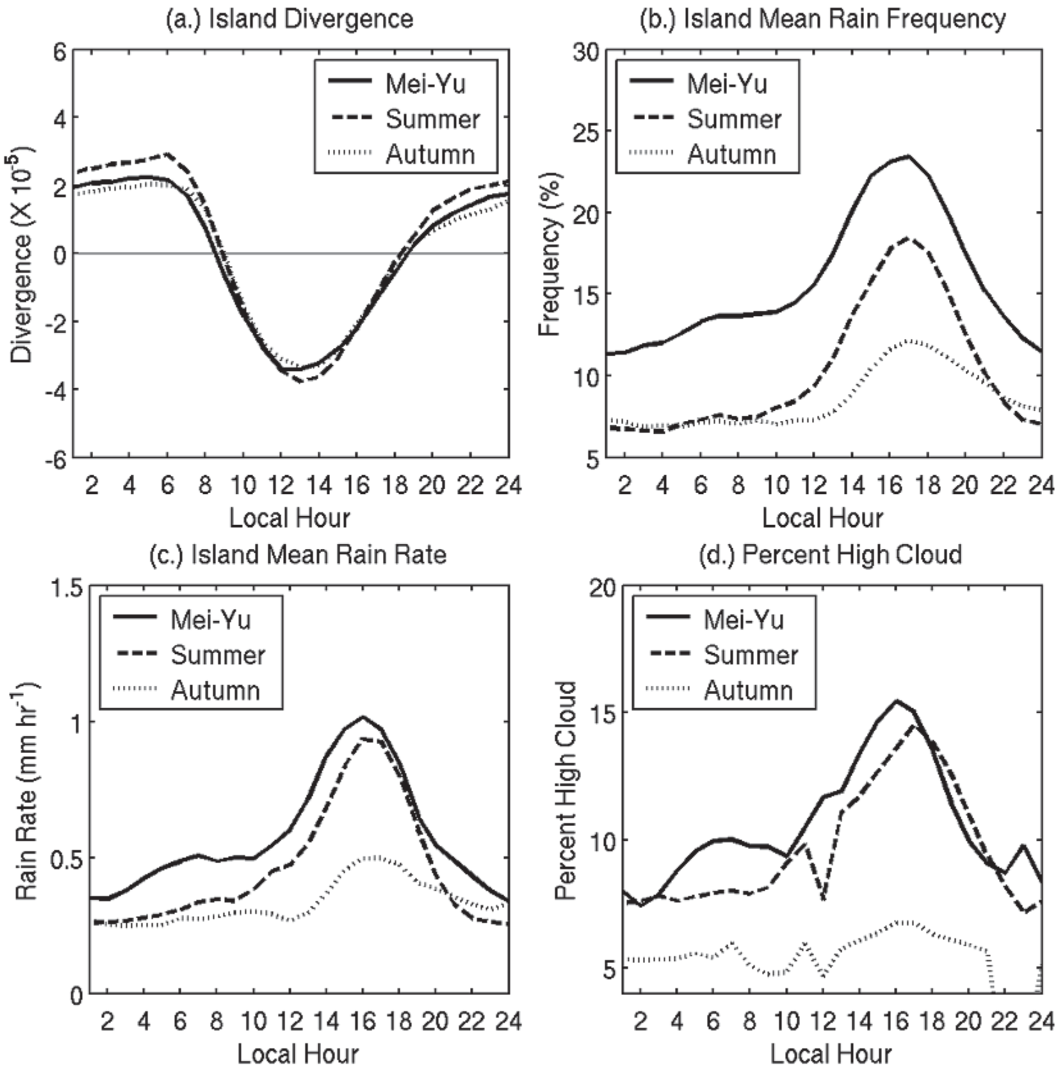

FIG. 9. (a) Mean hourly island divergence within the integration path in Fig. 3, (b) hourly rainfall frequency averaged over all stations, (c) hourly rain rate averaged over all stations, and (d) hourly percent coverage of 235-K cloud tops in the vicinity of Taiwan. Note that in (d) there are missing data for hours 12 and 23.

discussed later, the maximum morning rainfall occurrences over the west and northwest parts of Taiwan are associated with disturbed weather periods during the passage of mei-yu fronts. The weak early-morning rainfall maximum over southwestern Taiwan (Figs. 11a,b) is apparently caused by rain showers embedded within the south-southwesterly monsoon flow. These rainshowers drift inland and are enhanced by the convergence between the offshore flow (Fig. 6) and the decelerating incoming monsoon flow. Over the northern coast, weak early-morning rainfall maximum mainly occurs under postfrontal flow as a result of convergence between decelerating northeasterly flow and the offshore flow.

During the evening transition, most stations on the east side of the island experience evening rainfall maxima (Figs. 11c,d). Because of the westerly vertical shear (Fig. 1), remnant convection from the afternoon maximum over the mountainous terrain is likely to move eastward bringing rain to the southeastern side of Taiwan, where the terrain is lower, in the evening (Figs. 11c,d). It may be enhanced by local convergence between the northerly winds along the coast and the deflected southwesterly flow around the southern tip of Taiwan.

b. Diurnal cloud patterns

At night (0200 LT), deep convective clouds with cloud-top temperatures <235 K are infrequent (5%–10%) with maximum occurrence (>10%) over the ocean south of Taiwan, where the southwest monsoon flow is prevalent. The cold cloud frequencies south of Taiwan

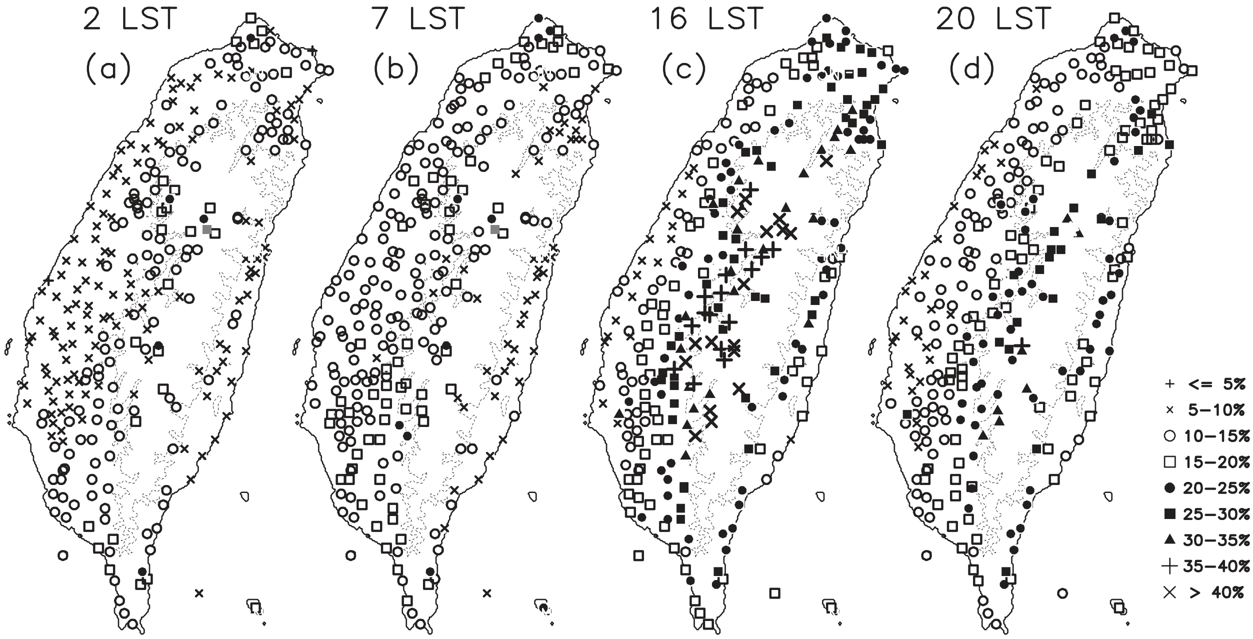

FIG. 10. Hourly rainfall frequencies (%) for selected times during the mei-yu for 1997–2002. The 1000-m terrain contour is drawn. The rainfall frequencies are the percentage of all observations ending on the particular hour that had measurable rainfall (>0.5 mm).

exceed 10% throughout the diurnal cycle (Fig. 12). North of Taiwan, postfrontal northeasterlies are common with suppressed deep convection (Chen 1993). Along the northern coast, there is no early-morning local maximum in cold cloud (Fig. 12b). As discussed earlier, the early-morning rainfall maximum there (Figs. 11a,b) mainly occurs under relatively stable postfrontal northeasterly flow. The low cold cloud frequencies over land (<10%) at night suggest that rainfall over land at night is mainly from scattered showers rather than deep convection.

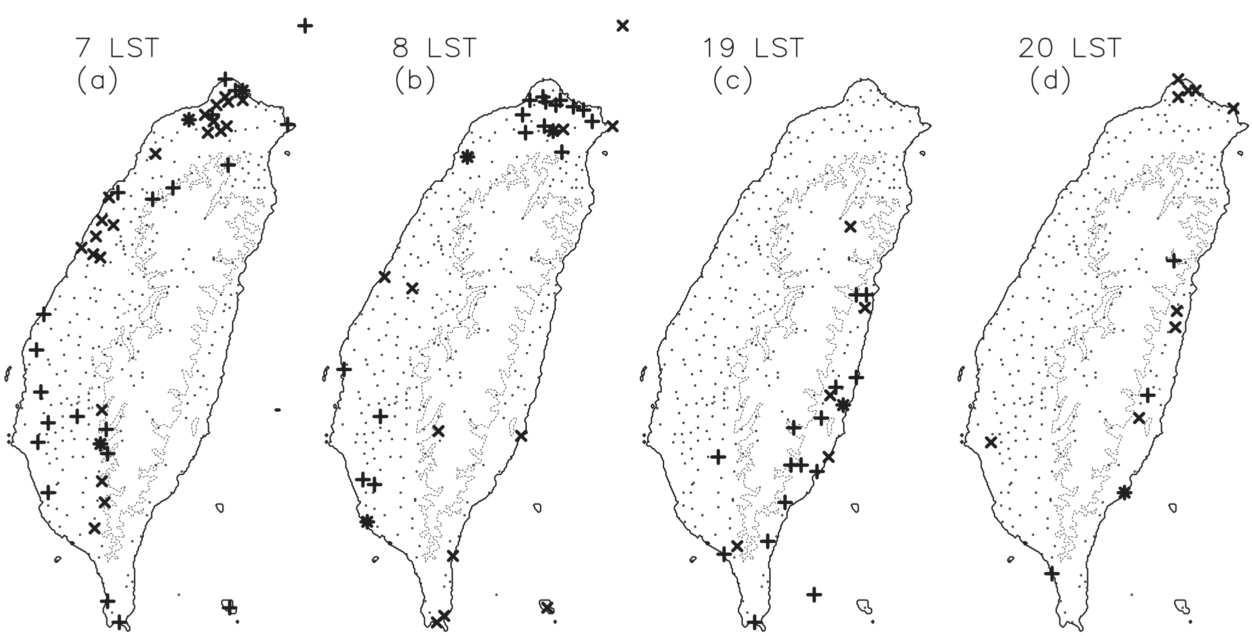

FIG. 11. The stations with relative rainfall frequency (plus sign) and rainfall rate (multiplication sign) maxima during the morning and evening transition, mei-yu. Stations with asterisks have both rainfall frequency and rainfall-rate maxima. The dots represent stations with neither rain frequency nor rain-rate maxima at the particular hour. The terrain CI is 1000 m.

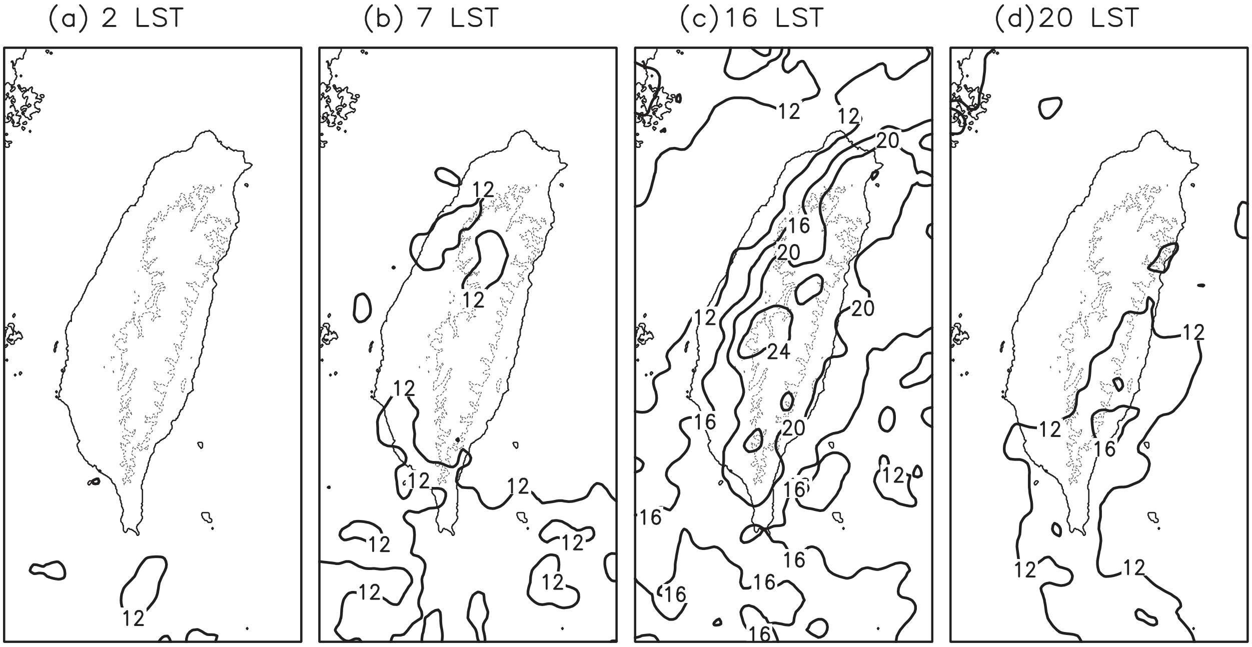

FIG. 12. Frequencies (%) of brightness temperatures below 235 K during the mei-yu for 1997–2002. The terrain CI is 1000 m. Nine-point smoothing has been applied twice. The CI is 4% starting with 12%.

In the afternoon, high cloud frequencies increase to above 20% (Fig. 12c) associated with the afternoon convection. The upper-level anvils are advected northeastward by the upper-level winds. High cloud frequencies off the southwestern coast upstream also have an afternoon maximum (>16%). In the evening, the maximum in cold cloud coverage is east of Taiwan (Fig. 12d) with a maximum over the southeastern coast consistent with the observed evening rainfall maximum there. Note that, even though a north–south cold cloud axis has been advected east of the ridge axis of the CMR by the upper-level westerly flow, frequent rainfall occurrences continue on the western and southwestern windward slopes in the early evening and diminish in the late evening (Fig. 10d).

The rainfall maxima observed on the west and northwest of Taiwan during the early morning is related to a maximum in high cloud occurrences that does not occur in summer and autumn (Fig. 13). The rainfall maximum is related to an axis of enhanced cold cloud frequencies that appears (>10%) in the Taiwan Strait around 0400 LT (Fig. 14a) and evolves into well-defined convective cloud maximum axis along the coast by 0600 LT (Fig. 14b). In the early morning, this high cloud axis continues to move inland (Fig. 14c).

The axis of high cloud frequencies over the northwest coast does not seem to be a regular day-to-day occurrence. Enhanced early-morning convection has also been observed over the Taiwan Strait from TRMM data by Krishtawal and Krishnamurti (2001). Furthermore, they found that during May and June 1998, the morning rainfall occurred in distinct ''surges'' while the afternoon rainfall was more regular. Yeh and Chen (1998) found that during TAMEX, more than 80% of rainfall over northwest Taiwan occurred during frontal passages. Under a strong southwest flow in the prefrontal environment, a mesoscale barrier jet frequently occurs along the northwest coast of Taiwan (Chen and Chen 1995; Chen and Li 1995; Li and Chen 1998), where the orographic blocking creates a windward ridge–leeside trough pattern (Chen et al. 1989; Trier et al. 1990; Chen and Hui 1992). The convergence zone between the barrier jet and the southwest monsoon flow and/or frontal wind shift line is a favored area for deep convection (Li et al. 1997; Yeh and Chen 2002, 2003). Also, the barrier jet serves to transport low-level moisture from south of Taiwan to the area of enhanced convergence. The barrier jet is most significant in the early morning as the mei-yu front approaches. Furthermore, the offshore flow is the strongest in the early morning, providing additional boundary layer convergence (Li et al. 1997).

In the early morning, high cloud frequencies offshore of the southwest coast and south of Taiwan are more frequent in the mei-yu than other two regimes (Fig. 14). It appears that mesoscale convective systems are frequently embedded within the southwest monsoon flow in the mei-yu. Furthermore, the convective activities are

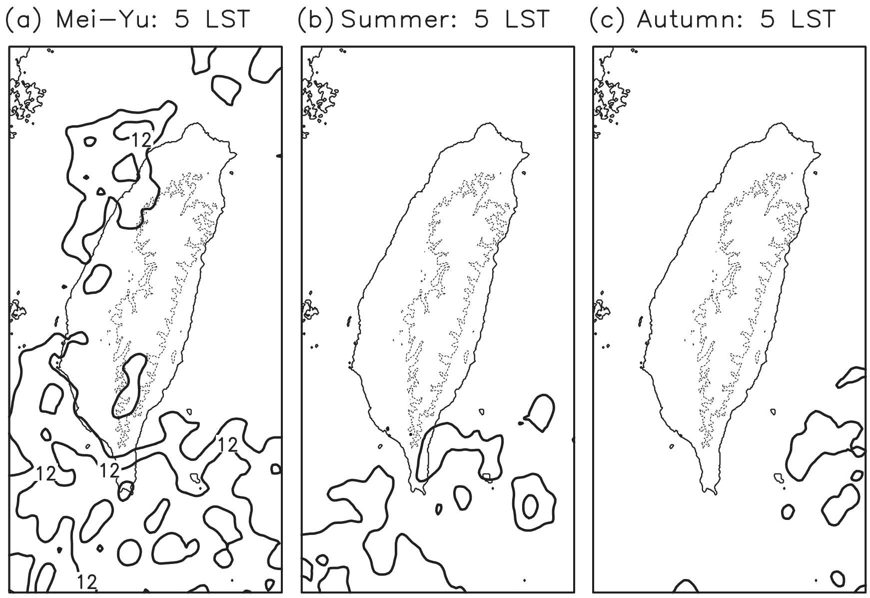

FIG. 13. Frequencies (%) of brightness temperatures below 235 K at 0500 LST during the (a) mei-yu, (b) summer, and (c) autumn for 1997–2002. The terrain CI is 1000 m. Nine-point smoothing has been applied twice. The CI is 2% starting with 10%.

enhanced by flow deceleration upstream off the southwest coast as a result of orographic blocking.

5. Summer

a. Diurnal rainfall patterns

Throughout the diurnal cycle most stations have lesser rainfall occurrences in summer than in the mei-yu (Figs. 4b and 9b). At night, without the presence of synoptic disturbances, rainfall occurrences are infrequent (<10%) except over a small area over windward south-southwestern Taiwan (Fig. 15a). In the early morning, in sharp contrast to the mei-yu, rainfall frequencies over the entire island are less than 10% except over southwestern Taiwan (Fig. 15b). The weak early-morning rainfall maximum over southwestern Taiwan is apparently caused by rain showers embedded within the south-southwesterly monsoon flow. These rain showers drift inland and are enhanced by the convergence between the offshore flow (Fig. 7a) and the decelerating incoming monsoon flow. At 1600 LT, rainfall frequencies are greater than 20% over southwestern Taiwan, western slopes, and northeastern slopes with the highest values exceeding 35%–40% over the southwestern windward slopes of the CMR (Fig. 15c) because of the development of onshore–upslope flow in the afternoon hours (Fig. 7c). At 2000 LT, the rainfall frequencies are still elevated over the mountainous interior, the southwestern windward side, and the northeastern slopes (Fig. 15d).

In summer, only a few stations over southwestern Taiwan have weak maximum rainfall occurrences during the morning transition (Figs. 16a,b). Without a frequent northeast–southwest cloud band and the prefrontal

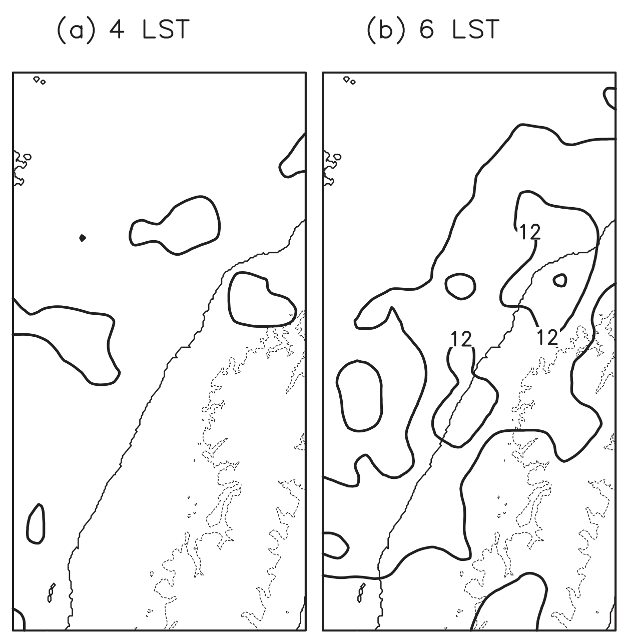

FIG. 14. Frequencies (%) of brightness temperatures below 235 K during the mei-yu for 1997–2002. The terrain CI is 1000 m. Nine-point smoothing has been applied twice. The CI is 2% starting with 10%.

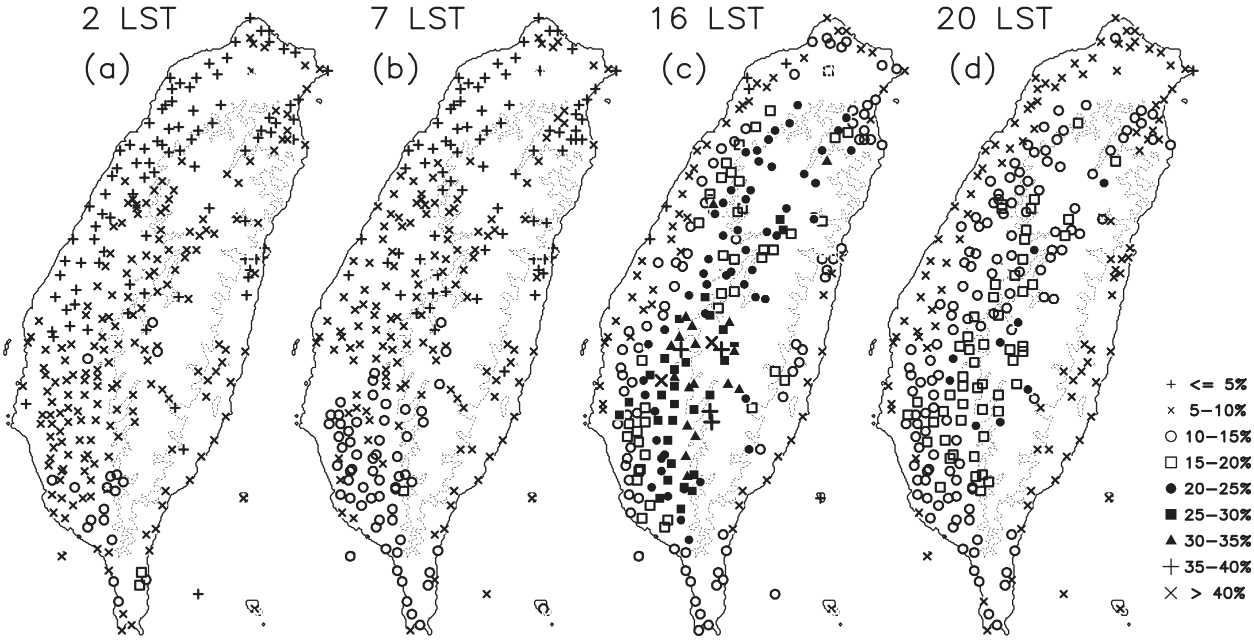

FIG. 15. As in Fig. 8, but for summer.

strong southwesterly flow as found during the mei-yu regime, there are no significant morning rain maxima on the northwest and west Taiwan as compared with the mei-yu. The occurrences of the morning rainfall maximum over western Taiwan noted by Chen et al. (1999) and Krishtawal and Krishnamurti (2001) do not occur in summer. Furthermore, under the weak summer south-southwesterly monsoon flow, northern-northeastern Taiwan is always on the lee side, in contrast to the postfrontal northeasterly flow during the mei-yu. Thus, the weak early-morning maximum rainfall occurrences due to the convergence between the postfrontal northeasterly flow and the offshore flow along the northern and northeastern coasts found in mei-yu (Figs. 11a,b) are also absent in summer (Figs. 16a,b).

Many stations on the west side of Taiwan have their rainfall maxima during the evening transition (Figs. 16c,d). There is a tendency for the location of the evening rainfall maximum to move westward from the mountainous interior to the coast between 1800 and 210 LT. There are two factors that may explain the evening rainfall maximum on the west coast of Taiwan. First, in many cases, the outflow boundaries from storms over the mountainous interior may initiate secondary convection farther west. Also, anvils from the interior convection, with mainly stratiform rain, would move primarily westward under the environmental easterly shear configuration (Fig. 1b). This is in sharp contrast to the mei-yu, in which the evening rainfall maxima occur over the east-southeast parts of Taiwan as remnants of orographically rain-showers move eastward due to westerly vertical wind shear.

b. *Diurnal cloud patterns*

As in the mei-yu, high clouds peak in the afternoon throughout the Taiwan area (Fig. 17). However, the maximum cold cloud frequency is located over the western coastal plain (Fig. 17c) well west of the location of maximum rainfall occurrences (Fig. 15c). Unlike the mei-yu, cold clouds in summer occur primarily west of the area of peak rainfall over the mountainous interior in the afternoon and early evening. The high clouds associated with the orographic showers within the mountain interior are advected westward by the upper-level northeasterly winds from the areas of convection to the southwestern coastal plain. Furthermore, over the ocean south of Taiwan, high cloud frequencies are slightly higher in the late afternoon (Fig. 17c) than other time periods during the day.

6. Autumn

a. *Diurnal rainfall patterns*

It is during autumn that the strongest contrast in rainfall occurrences between the windward and leeward sides is observed, for it is this regime that has the strongest persistent environmental winds (Figs. 1 and 2) with relatively stable stratification (Table 1). At 0200 LT, west of the CMR, rainfall frequencies were below 5%, whereas

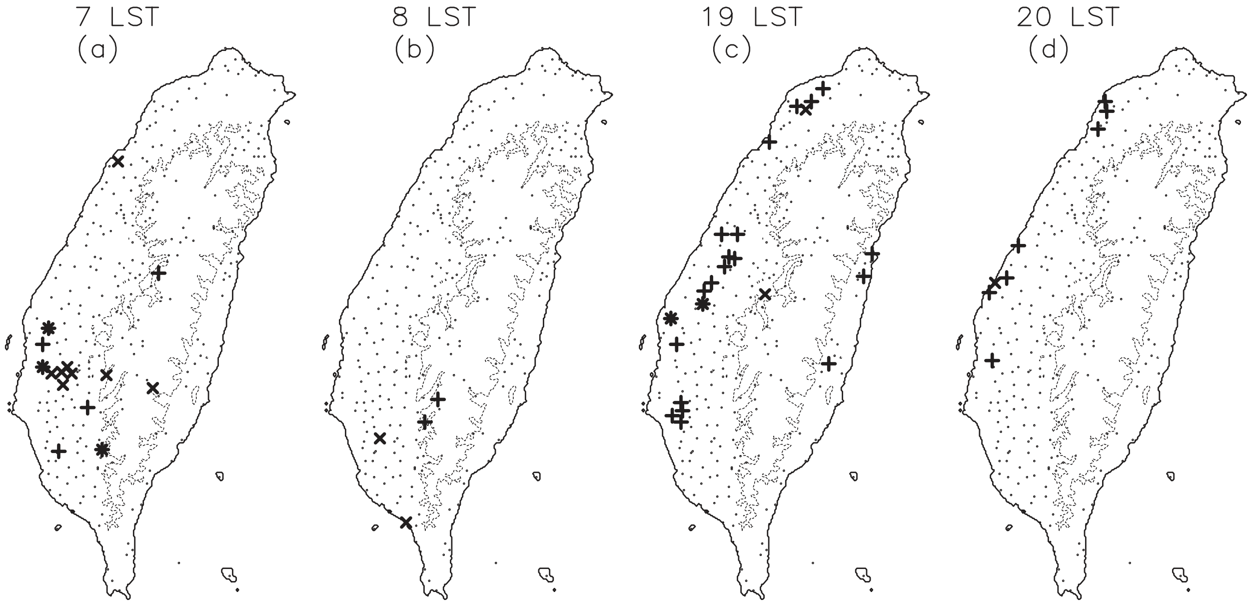

FIG. 16. As in Fig. 9, but for summer.

east of the CMR, rainfall frequencies were about 10%–25%, with the highest values in northeastern Taiwan in the afternoon hours (Fig. 18). This northeast/southwest contrast is a persistent feature throughout the diurnal cycle. The spatial contrast in rainfall occurrence in autumn suggests that most of the rainfall is generated by orographic uplift and enhanced by a stronger upslope wind component in the afternoon hours. On the lee side (southwest) of Taiwan, rainfall mainly occurs on the leeside slopes in the afternoon (Fig. 18c).

In the early morning, the weak early-morning maximum rainfall occurrences over western Taiwan coast and many stations inland found during mei-yu and southwestern Taiwan found in summer are absent as

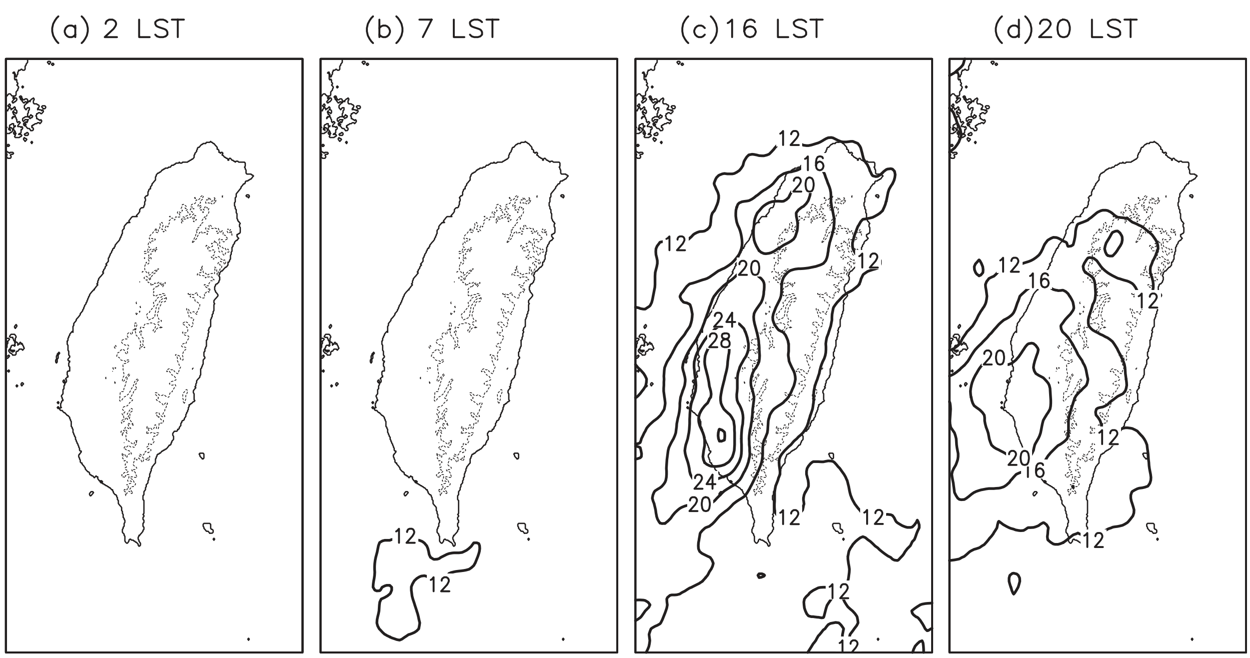

FIG. 17. As in Fig. 10, but for summer.

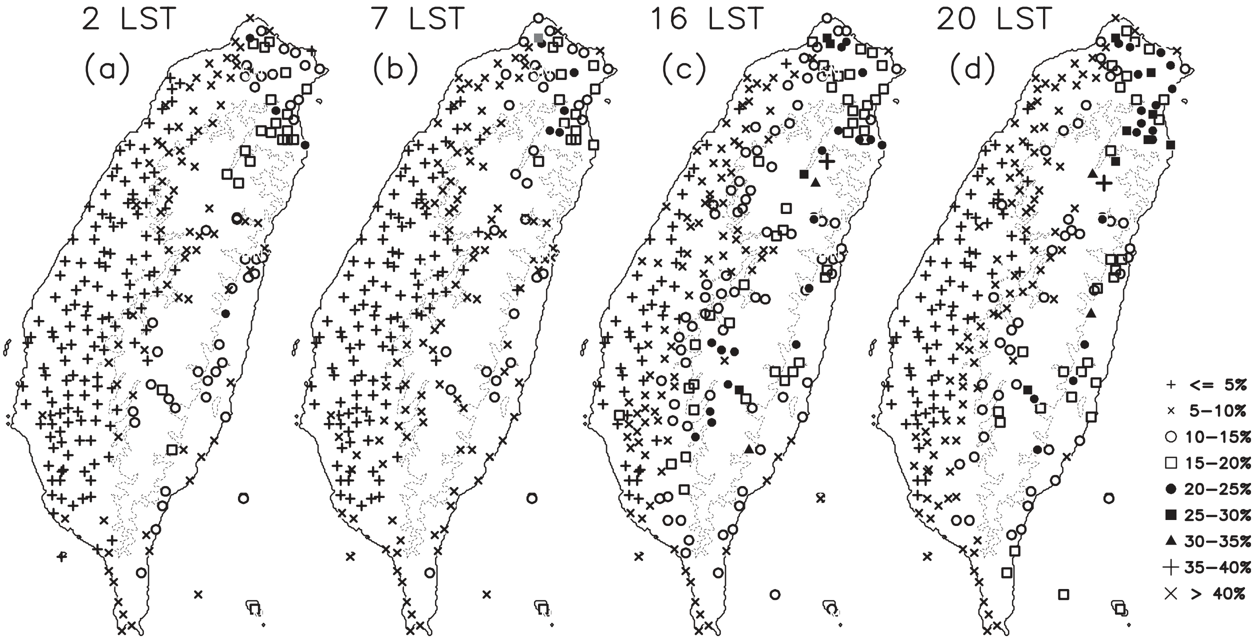

FIG. 18. As in Fig. 8, but for autumn.

these regions are in the leeside areavs (Figs. 19). Weak early-morning maximum rainfall occurrences are observed over northern and northeastern Taiwan in autumn due to the convergence between the offshore flow and the northeasterly monsoon flow and orographic blocking.

During the evening transition, for the stations on the leeside slopes west of CMR, rainfall occurrences diminish as upslope winds subside, whereas on the windward side of the northeasterly monsoon flow, there is a tendency of increasing rainfall occurrences as the shallow orographic showers lingering on the windward (northeast) side continue to be enhanced by the offshore flow and the decelerating northeasterly flow.

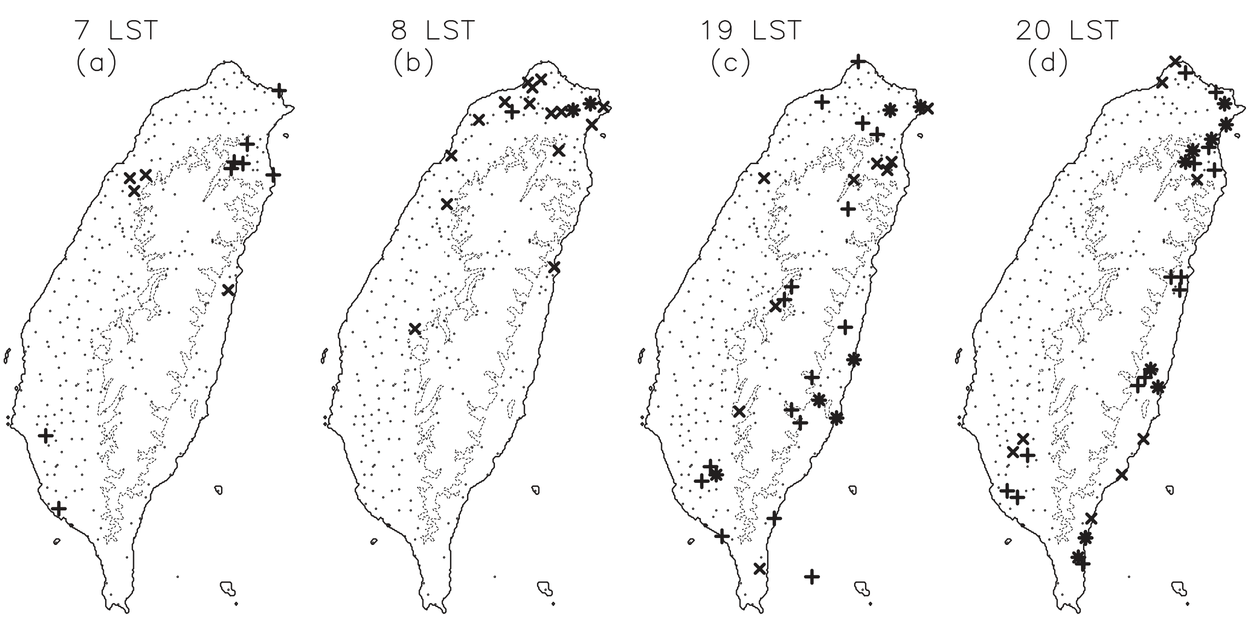

FIG. 19. As in Fig. 9, but for autumn.

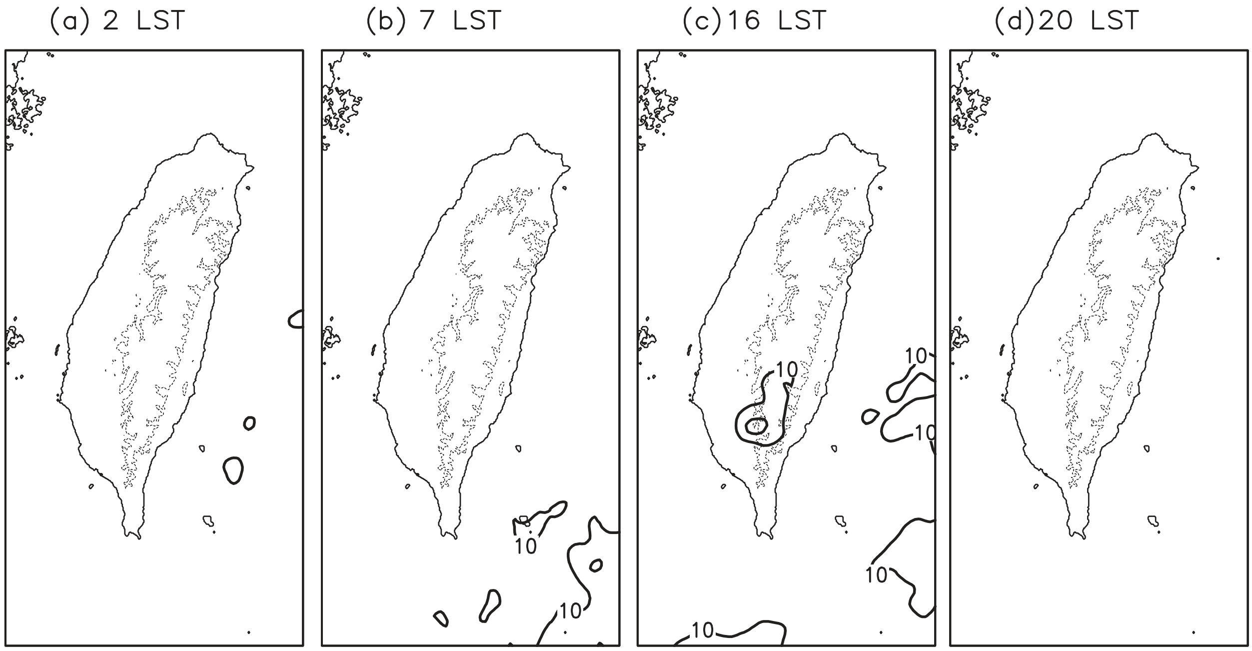

FIG. 20. Frequencies (%) of brightness temperatures below 235 K during the mei-yu for 1997–2002. The terrain CI is 1000 m. Nine-point smoothing has been applied twice. The CI is 2% starting with 10%.

b. *Diurnal cloud patterns*

In contrast to both the mei-yu and summer, autumn deep convective cloud frequencies are less than 10% throughout the diurnal cycle except in the afternoon over the a small area over the southwestern slopes of CMR (Fig. 20). This afternoon maximum (>10%) is collocated with the rainfall frequency maximum over the mountainous interior of southwestern Taiwan (Fig. 20c) without extensive anvils. This is related to the fact that the instability is the least in autumn among the three regimes (Table 1).

Over northeastern Taiwan there is no pronounced maximum in cold cloud occurrence, where the rainfall occurrences are more frequent than the other areas with an afternoon maximum. This suggests that most of the rainfall over northeastern Taiwan during autumn does not occur from deep convection, but from relatively shallow orographic showers.

7. Summary and conclusions

The diurnal cycle of winds, rainfall, and high clouds is investigated for three distinct rainfall regimes over Taiwan (Chen and Chen 2003): mei-yu (16 May–15 June), summer (16 July–31 August), and autumn (16 September–31 October) to highlight the factors that determine the island-scale weather under different large-scale conditions. In all three regimes, the mean surface diurnal winds are dominated by the daytime upslope–onshore flow and the nighttime downslope–offshore flow. The exception is along the northern Taiwan coast in autumn, where the northeasterly flow prevails throughout the diurnal cycle. The overall strength of the diurnal winds, as measured by island divergence, is similar under each regime. Even though the strongest insolation occurs in summer, the early-morning divergence and afternoon convergence are not significantly higher than for the mei-yu or autumn. For all three regimes, rainfall occurrences, rain rates, and cold cloud coverage are strongly modulated by the diurnal heating cycle with a pronounced late afternoon (~1600 LT) maximum.

For most stations, rainfall is most frequent in the mei-yu throughout the diurnal cycle as compared with other regimes because of the frequent arrival of mei-yu fronts from southern China. In the mei-yu, a distinct secondary rainfall maximum occurs in the early morning. Rainfall at late night and early morning is mainly due to drifting of rain showers inland and scattered orographic showers during mei-yu frontal passages. Rainfall often organizes into bands off the northwest coast, where the south-southwest barrier jet meets the prefrontal southwest flow. This occurs preferentially in the early morning because the atmosphere is more stable, which favors a strong barrier jet. Also, in the prefrontal environment strong southwest winds impinge on the CMR and are deflected northward, leading to the formation of the barrier jet. This distinctive phenomenon does not occur in summer (which lacks frontal passages with a strong prefrontal southwest flow) or autumn (which is dominated by stable northeast monsoon flow).

The summer conditions with light environmental winds and infrequent synoptic disturbances may be interpreted to represent the undisturbed diurnally induced island circulations. Summer is the period with the most significant daytime–nighttime contrast in rainfall occurrences. In summer, the afternoon convection over the western mountain slopes is most pronounced in summer. The atmosphere is most unstable in summer, and there are relatively few disturbances embedded in the environment flow to trigger convection. At night, there is little contrast between the mountains and coastal areas in terms of convective cloud frequencies (<10%). Rainfall at night is also infrequent (<10%) over land. The afternoon maximum in convective and cold cloud frequencies (>30%) occurs over the west-southwestern coastal plain, whereas the rainfall maximum is over the mountain slopes. It is apparent that the upper-level anvils associated with the afternoon convection are carried westward by the upper-level easterlies.

In autumn, the prevailing flow is northeast and the environment is more stable. Afternoon rainfall maxima from deep convection occur only over a very limited area of the southwest CMR slopes, where the northeast monsoon flow is blocked by the CMR. Afternoon maximum rainfall frequencies (>30%) occur in the north and east of the island on the windward side. However, cold cloud is infrequent (<10%) in these area. Most of the rainfall there is generated by orographic uplift and flow blocking enhanced by a stronger upslope flow component in the afternoon hours.

The stations with rainfall maxima during the transition periods have also been considered for each regime. The weak early-morning rainfall maximum is mainly related to the interaction between the prevailing winds and the island-induced airflow. During the mei-yu, the weak early-morning rainfall maximum over the northern coast mainly occurs under the postfrontal flow as a result of convergence between the decelerating northeasterly flow and the offshore flow. In the early morning, high cloud frequencies offshore of the southwest coast and south of Taiwan are more frequent in the mei-yu than other regimes. It appears that mesoscale convective systems are frequently embedded within the southwest monsoon flow in the mei-yu. Furthermore, the convective activities are enhanced by flow deceleration upstream off the southwest coast. In summer, weak early-morning rainfall maximum is observed over southwestern Taiwan related to the convergence between the offshore flow and the decelerating incoming southwest monsoon flow. In autumn, weak early-morning maxima occur on the northern and northeastern windward side due to orographic blocking and the convergence between the offshore flow and the northeast monsoon flow.

In the mei-yu and summer, weak evening rain maxima are related to remnant afternoon convection in the mountainous interior that is advected by the upper-level winds. In the mei-yu, with upper-level westerlies, the afternoon convection on the western windward slopes moves eastward resulting in weak evening rainfall maximum over southeastern Taiwan where the ridge axis of the Central Mountain Range is lower. It may be enhanced by local convergence between the northerly winds along the east and southeast coasts and the deflected southwesterly flow around the southern tip of Taiwan. In summer, with upper-level northeasterlies, the upper-level anvils are advected southwestward with weak evening rainfall maximum along the west and southwest Taiwan coasts. In autumn, rainfall frequencies over the southwestern lee side diminish, whereas on the windward side, some stations that recorded a weak evening maximum as the shallow orographic showers lingering on the windward side are enhanced by the convergence between the offshore flow and the decelerating incoming flow.

Acknowledgments. We thank Diana Henderson, who helped with editing the manuscript, and Prof. C.-S. Chen for comments and assistance. Dr. Robert Grossman and anonymous reviewers provided valuable feedback that greatly improved the manuscript. The ARMTS and routine surface data were obtained from the Central Weather Bureau. This research was supported by the National Science Foundation under Grant ATM-0140387. The authors also appreciate the support of the Pacific Disaster Center, Kihei, Hawaii; the U.S. Forest Service; and the U.S. Department of Agriculture under Cooperative Agreement 05-JV-11272165-015.

REFERENCES

Akaeda, K., J. Reisner, and D. Parsons, 1995: The role of mesoscale and topographically induced circulations initiating a flash flood observed during the TAMEX project. *Mon. Wea. Rev.,* **123,** 1720–1739.

Boyle, J. S., and G. T. J. Chen, 1987: Synoptic aspects of the wintertime East Asian monsoon. *Monsoon Meteorology,* C. P. Chang and T. N. Krishnamurti, Eds., Oxford University Press, 125–160.

Central Weather Bureau, 1995: *The Basic Information of Meteorological Observation Statistic* (in Chinese). 4th ed. Central Weather Bureau, 163 pp. [Available from the Central Weather Bureau, 64 Kung-Yun Rd., Taipei 100, Taiwan.]

Chen, C.-S., and Y.-L. Chen, 2003: The rainfall characteristics of Taiwan. *Mon. Wea. Rev.,* **131,** 1323–1341.

——, W.-S. Chen, and Z. Deng, 1991: A study of a mountain-generated precipitation system in northern Taiwan during TAMEX IOP 8. *Mon. Wea. Rev.,* **119,** 2574–2607.

——, Y.-L. Chen, C.-L. Liu, P.-L. Lin, and W.-C. Chen, 2007: Statistics of heavy rainfall occurrences in Taiwan. *Wea. Forecasting,* **22,** 981–1002.

Chen, T. C., M. C. Yen, J. C. Hsieh, and R. W. Arrit, 1999: Diurnal and seasonal variations of the rainfall measured by the automatic rainfall and telemetry system in Taiwan. *Bull. Amer. Meteor. Soc.,* **80,** 2299–2312.

Chen, X. A., and Y. L. Chen, 1995: Development of low level jets (LLJs) during TAMEX. *Mon. Wea. Rev.,* **123,** 1695–1719.

Chen, Y.-L., 1993: Some synoptic-scale aspects of the surface fronts over southern China during TAMEX. *Mon. Wea. Rev.,* **121,** 50–65.

——, and N. B.-F. Hui, 1992: Analysis of a relatively dry front during the Taiwan Area Mesoscale Experiment TAMEX. *Mon. Wea. Rev.,* **120,** 2442–2468.

——, and J. Li, 1995: Characteristics of surface airflow and pressure patterns over the island of Taiwan during TAMEX. *Mon. Wea. Rev.,* **123,** 695–716.

——, Y.-X. Zhang, and N. B.-F. Hui, 1989: Analysis of a surface front during the early summer rainy season over Taiwan. *Mon. Wea. Rev.,* **117,** 909–931.

Dairaku, K., S. Emori, and T. Oki, 2004: Rainfall amount, intensity, duration, and frequency relationships in the Mae Chaem watershed in southeast Asia. *J. Hydrometeor.,* **5,** 458–470.

Fu, R., A. D. Del Genio, and W. M. Rossow, 1990: Behavior of deep convective clouds in the tropical Pacific deduced from ISCCP radiances. *J. Climate,* **3,** 1129–1152.

Grossman, R. L., and D. R. Durran, 1984: Interaction of low-level flow with the Western Ghat Mountains and offshore convection in the summer monsoon. *Mon. Wea. Rev.,* **112,** 652–672.

Hsu, J., 1998: ARMTS up and running in Taiwan. *Vaisala News,* **146,** 24–26.

Johnson, R. H., and J. F. Bresch, 1991: Diagnosed characteristics of precipitation systems over Taiwan during the May-June 1987 TAMEX. *Mon. Wea. Rev.,* **119,** 2540–2557.

Kuo, Y. H., and G. T.-J. Chen, 1990: Taiwan Area Mesoscale Experiment: An overview. *Bull. Amer. Meteor. Soc.,* **71,** 488–503.

Krishtawal, C. M., and T. N. Krishnamurti, 2001: Diurnal variation of summer rainfall over Taiwan and its detection using TRMM observations. *J. Appl. Meteor.,* **40,** 331–344.

Li, J., and Y.-L. Chen, 1998: Barrier jets during TAMEX. *Mon. Wea. Rev.,* **126,** 959–971.

——, ——, and W.-C. Lee, 1997: Analysis of a heavy rainfall event during TAMEX. *Mon. Wea. Rev.,* **125,** 1060–1082.

Lin, Y.-J., H. Shen, T.-C. C. Wang, Z.-S. Deng, and R. W. Pasken, 1990: Characteristics of a subtropical squall line determined from TAMEX dual-Doppler data. Part II: Dynamic and thermodynamic structures and momentum budgets. *J. Atmos. Sci.,* **47,** 2382–2399.

Murakami, T., 1958: The sudden change of upper westerlies near the Tibetan Plateau at the beginning of the summer season. *J. Meteor. Soc. Japan,* **36,** 239–247.

Ogura, Y., and M. Yoshizaki, 1988: Numerical study of orographic-convective precipitation over the Eastern Arabian Sea and the Ghat Mountains during the summer monsoon. *J. Atmos. Sci.,* **45,** 2097–2122.

Oki, T., and K. Musiake, 1994: Seasonal change of the diurnal cycle of precipitation over Japan and Malaysia. *J. Appl. Meteor.,* **33,** 1445–1463.

Overland, J. E., and N. A. Bond, 1995: Observations and scale analysis of coastal wind jets. *Mon. Wea. Rev.,* **123,** 2934–2941.

Ramage, C. S., 1952: Diurnal variation of summer rainfall over east China, Korea, and Japan. *J. Meteor.,* **9,** 83–86.

——, 1971: *Monsoon Meteorology*. Academic Press, 296 pp.

Smolarkiewicz, P. K., R. M. Rasmussen, and T. L. Clark, 1988: On the dynamics of Hawaiian cloud bands: Island forcing. *J. Atmos. Sci.,* **45,** 1872–1905.

Sun, W.-Y., and J.-D. Chern, 1993: Diurnal variation of lee vortices in Taiwan and the surrounding area. *J. Atmos. Sci.,* **50,** 3404–3430.

——, ——, C.-C. Wu, and W.-R. Hsu, 1991: Numerical simulation of mesoscale circulation in Taiwan and surrounding area. *Mon. Wea. Rev.,* **119,** 2558–2573.

Tao, S., and L. Chen, 1987: A review of recent research on the East Asian monsoon in China. *Monsoon Meteorology,* C. P. Chang and T. N. Krishnamurti, Eds., Oxford University Press, 60–92.

Teng, J.-H., C.-S. Chen, T.-C. C. Wang, and Y.-L. Chen, 2000: Orographic effects on a squall line system over Taiwan. *Mon. Wea. Rev.,* **128,** 1123–1138.

Trier, S. B., D. B. Parsons, and T.-J. Matejika, 1990: Observations of a subtropical cold front in a region of complex terrain. *Mon. Wea. Rev.,* **118,** 2449–2470.

Wang, T.-C. Chen, Y.-J. Lin, H. Shen, and R. W. Pasken, 1990: Characteristics of a subtropical squall line determined from TAMEX dual-Doppler data. Part I: Kinematic structure. *J. Atmos. Sci.,* **47,** 2357–2381.

Yeh, H.-C., and Y.-L. Chen, 1998: Characteristics of rainfall distributions over Taiwan during the Taiwan Area Mesoscale Experiment (TAMEX). *J. Appl. Meteor.,* **37,** 1457–1469.

——, and ——, 2002: The role of offshore convergence on coastal rainfall during TAMEX IOP 3. *Mon. Wea. Rev.,* **130,** 2709–2730.

——, and ——, 2003: Numerical simulations of the barrier jet over northwestern Taiwan during the mei-yu season. *Mon. Wea. Rev.,* **131,** 1396–1407.